Catalytic Hydrogen Production from Methane Partial Oxidation: Mechanism and Kinetic Study

Osman Ahmed, A. O. (2020). Catalytic Hydrogen Production from Methane Partial Oxidation: Mechanism and Kinetic Study. *Chemical Engineering and Technology*, 1–9. [Chem. Eng. Technol.2020,43, No. 00]. https://doi.org/10.1002/ceat.201900339

Published in:
Chemical Engineering and Technology

Document Version:
Peer reviewed version

Queen's University Belfast - Research Portal:
Link to publication record in Queen's University Belfast Research Portal

Catalytic hydrogen production from methane partial oxidation: mechanism and kinetic study mini-review

Ahmed I. Osman [a]*

[a] School of Chemistry and Chemical Engineering, Queen's University Belfast, Belfast BT9 5AG, Northern Ireland, UK

Corresponding Authors: Dr. Ahmed I. Osman

Email: aosmanahmed01@qub.ac.uk

Address: School of Chemistry and Chemical Engineering, Queen's University Belfast, David Keir Building, Stranmillis Road, Belfast BT9 5AG, Northern Ireland, United Kingdom

Fax: +44 2890 97 4687

Tel.: +44 2890 97 4412

Abstract

Herein, this mini review investigates the multifunctional potential of a transition and noble metal catalyst supported on either a single support or combined oxide support in the catalytic partial oxidation of methane (CPOM). Also highlighted is the close interaction and interfacial area between the metal, reducible oxide and acidic support, which are crucial for the low-temperature CPOM reaction. The effect of the catalyst component and its preparation methods were considered herein. Their impact on the catalytic performance and stability on the CPOM reaction was evaluated. The two main mechanisms of CPOM; direct partial oxidation (DPO) and the combustion and reforming reaction (CRR) mechanism was also covered along with the most recent kinetic studies. Finally, the deactivation of the CPOM catalysts was studied in term of coke and carbon deposition along with the CO poisoning.

Keywords: Methane, Partial oxidation, Zeolite support, Oxygen carrier, Nickel, Hydrogen production.

1. Introduction

Methane is the simplest, most symmetrical occurring hydrocarbon and is the main component of natural gas (>88 vol.%) [1]. It is also generated from renewable resources such as biogas (50-70 vol.%), which is a valuable resource for energy generation and chemical feedstock supply [1, 2]. Combustion, in general, is an exothermic redox chemical reaction between a fuel and an oxidant, which is triggered by activation energy in the form of heat or a flame. Methane total combustion with excessive O_2 to CO_2 and H_2O generates a large amount of energy (802.3 $kJ.mol^{-1}$); with lower greenhouse gas emissions (GHG) compared to that of other hydrocarbon fuels [3] (Eq. 1). While its partial combustion using a stoichiometric ratio of 2:1 (CH_4 : O_2) produces synthesis gas (syngas); a mixture of CO and H_2 as shown in Eq. 2. Hydrogen can be produced after the removal of CO using the water gas shift reaction (WGSR).

$$CH_4 + 2O_2 \longrightarrow CO_2 + 2H_2O \quad \Delta H° = -802.3\ kJ.mol^{-1} \qquad \text{Eq. 1}$$

$$CH_4 + {}^1/_2O_2 \longrightarrow CO + 2H_2 \quad \Delta H° = -36\ \ kJ.mol^{-1} \qquad \text{Eq. 2}$$

Catalytic partial oxidation of methane (CPOM) requires high-temperature (>800 °C) which produces alongside CO and H_2 as main products: carbon as soot or ash, CO_2 and H_2O as by-products [1]. This means that coke formation is thermodynamically favoured at relatively high temperature, thus reducing the yield of syngas [4-6]. To overcome the catalyst deactivation by coke formation, additional catalyst is needed to maintain production throughout regeneration cycles. Others general byproducts of the combustion process are nitrogen oxide (NO_x), sulfur oxide (SO_x) and others particulates. Usually, fuel combustion reactions at high temperatures under air atmosphere (78 vol.% N_2) generates NO_x, since N_2 combustion is thermodynamically favourable at high temperature, but not at low temperatures. The release of such emissions is positively correlated to adverse health and environmental effects [7]. Hence, the production of syngas at low-temperature range offers significant financial and environmental advantages,

67 including lower energy requirements, materials costs as well as reduced formation of NO_x
68 emissions.
69 Syngas is generally formed from the large scale steam reforming of hydrocarbons and is used for
70 a variety of applications including the manufacture of fuels and feedstocks and the production of
71 hydrogen [8, 9]. However, with increasing utilisation of stranded and small scale sources of
72 methane such as farms and AD plants in remote areas as well as decreasing acceptance of flaring
73 at source, development of a catalyst to allow CPOM to syngas on a smaller scale is desired [4].

74 **2. Why partial oxidation is the most suitable reforming reaction for liquid fuels**
75

76 There are three main reforming routes to produce syngas from methane which are dry reforming,
77 steam reforming and oxy reforming (partial oxidation). The first two reforming routes are highly
78 endothermic processes (Eq. 3-4), along with the fact they are both prone to coke formation and
79 eventually catalyst deactivation. However, partial oxidation is a mildly exothermic reaction as
80 shown in Eq. 2.

81 $CH_4 + H_2O \rightarrow CO + 3H_2$ $\Delta H° = 206$ kJ.mol^{-1} Eq. 3

82 $CH_4 + CO_2 \rightarrow 2CO + 2\ H_2$ $\Delta H° = 247$ kJ.mol^{-1} Eq. 4

83 More importantly, for the production of liquid fuel such as methanol and consequently, the
84 biofuel dimethyl ether (DME) as shown in Eq. 5, a H_2 : CO ratio of 2 in the produced syngas is
85 required [10]. Interestingly, partial oxidation offers that ratio requirement, whereas steam and
86 dry reforming produce syngas with a ratio of 3 and 1, respectively. Thus, steam reforming is
87 more appropriate for hydrogen production, combining with WGSR to remove the CO produced
88 [11]. While dry reforming with a ratio of 1 is appropriate for dimethyl ether production in one
89 single step at high pressure as shown in Eq. 6.

90 $2CH_3OH \longleftrightarrow CH_3OCH_3 + H_2O$ Eq. 5

$3CO + 3H_2 \longleftrightarrow CH_3OCH_3 + CO_2$ Eq. 6

Partial oxidation of methane is also the most appropriate reforming process for the Fischer–Tropsch process, where a H_2 : CO ratio of 2 in the produced syngas is also required [4, 12, 13].

3. Types of metal catalysts

There are mainly two types of metal catalysts in CPOM reaction which are transition or noble metals catalysts as shown below.

3.1 Transition metal catalysts

Among the transition metal catalysts, nickel is recognised as one of the cheapest and most active catalysts. However, it is prone to carbon deposition which poisons and consequently, deactivates the catalyst [13]. Thus, numerous work in the literature is devoted to using Ni-based catalysts with reduced carbon deposition [14]. One example of suppressing the carbon deposition is to use reducible oxide support such as CeO_2 or ZrO_2 as single support or CeO_2-ZrO_2 as combined oxide support. Other oxygen supports that were also used were TiO_2 and La_2O_3, where the lattice oxygen within the oxide support oxidise any carbon deposited on the surface of the catalyst during CPOM reaction [15-21]. The typical temperature range for Ni-based catalysts in CPOM reaction is 550-850 °C. The three biggest challenges with Ni catalysts in CPOM reaction are the high temperature required for high syngas yield (>850 °C), high selectivity of CO_2 and the coke formation. For instance, Ni supported on a single support such as Ni/CeO_2 catalyst showed a temperature at 50% conversion ($T_{50\%}$) of 720 °C. While on combined oxide support such as Ni/CeO_2/La_2O_3 catalyst, $T_{50\%}$ was at 675 °C using a gas hourly space velocity (GHSV) of 60,000 $mL.g^{-1}.h^{-1}$. Recently, Ni/CeO_2-ZrO_2/ZSM-5 (80) catalyst showed enhanced catalytic activity, where $T_{50\%}$ was at 400 °C using WHSV of 63,000 $mL.g^{-1}.h^{-1}$ [13]. That catalyst showed also good stability over 25 hours reaction stream at reaction temperatures of both 400 and 700 °C,

116 respectively. Wang et al. improved the coking resistance of Ni-based catalyst along with
117 synthesising small Ni particles by doping Praseodymium oxide [22] in the autothermal reforming
118 of CH_4 reaction. Furthermore, the Pr loading improved the catalytic activity along with the
119 H_2:CO molar ratio.

120 *3.2 Noble metal catalysts*
121

122 Several noble catalysts have been used in CPOM reaction, especially group VIII-X (8-10) metals.
123 For instance: rhodium (Rh), ruthenium (Ru), palladium (Pd), Lanthanum (La) and platinum (Pt)
124 [1, 4-6, 17, 23-31], where rhodium showed good activity [17, 23-26]. It was reported that Rh is
125 more selective to syngas production (CO and H_2) than that of Pt in CPOM reaction in the
126 corresponding catalysts of Rh/α-Al_2O_3 and Pt/α-Al_2O_3, respectively [26]. However, a high
127 reaction temperature was still required (1000 °C) for Rh/α-Al_2O_3 catalyst to achieve 37%
128 methane conversion at 6 vol.% CH_4 in the reaction feed. On the other hand, Rh/$CeZrO_2$ catalyst
129 showed 95% conversion at a reaction temperature of 750 °C (3.3% CH_4 in the feed). Lately,
130 Rogozhnikov et al.[32] prepared Rh/θ-Al_2O_3/FeCr alloy in the form of a wire mesh composite
131 catalyst for CPOM reaction. They reported that the catalyst showed good performance with
132 equilibrium product distribution and syngas productivity of 56.7 $m^3.L.cat^{-1}.h^{-1}$ (s.c.) at 800 °C at
133 23.5 vol.% CH_4 in the reaction feed (GHSV of 80000 h^{-1}) [32]. In a recent study, Alvarez-Galvan
134 et al.[33] studied the impact of doping Rh on Ni-based catalyst in CPOM reaction. It is not
135 surprising that unmodified Ni-based catalyst suffered from fast deactivation. However, they
136 found out that Rh favours Ni reduction, which led to an improvement in the conversion and yield
137 alongside 80% conversion at 750 °C (29.5% CH_4 in the feed) [33]. Boukha et al.[34] studied the
138 role of the Rh particle size in hydroxyapatite catalysts for CPOM reaction where Rh(x)/HAP
139 catalysts showed high coke-resistance from a stability test which lasted for 30 hours at 700 °C.

140 They found the interaction between the Rh and the TCP support had a negative impact on the
141 performance of the catalyst during CPOM reaction.

142 Ru metal was included in a combination of Co-Ni-Ru catalyst for CPOM reaction and showed
143 98% conversion along with high CO selectivity (94%) [35] at 10000 h^{-1}. La metal is usually used
144 to promote methane total oxidation (MTO) into CO_2 and H_2O, where Ni is added as a promoter
145 to convert those products into syngas [29]. Thus, Ni and La were used as a bimetallic catalyst in
146 CPOM reaction. For instance, Pantaleo et al. [5] used 5%Ni/CeO_2-La_2O_3 catalyst in CPOM
147 reaction with $T_{50\%}$ found to be at 675 °C at GHSV of 60000 $mL.g^{-1}.h^{-1}$. Re metal is also used to
148 promote the Ni-based catalyst. For instance, Cheephat et al. [36] studied the promotion effect of
149 Rh or Re on Ni/Al_2O_3 catalyst. They found out that Re-Ni/Al_2O_3 showed high stability with
150 slight deactivation in H_2 yield after 18 hours of operation.

151 **4. Effect of catalyst components**
152

153 As discussed above, the most common active noble metal is rhodium, whilst for transition metals
154 it is nickel. Accompanied by the metal content, acidic catalyst supports such as Al_2O_3, ZSM-5
155 and oxygen support materials (TiO_2, CeO_2-ZrO_2) play a crucial role in CPOM reaction. Ni-based
156 catalysts were prepared on different supports: acidic (Al_2O_3), oxygen storage (CeO_2) and basic
157 (MgO); where Ni-Al_2O_3 and Ni-CeO_2 catalysts showed better activity and stability than that of
158 Ni-MgO [33]. This was explained due to the higher surface area of Ni nanoparticles on the
159 alumina support and the existence of oxygen vacancies in the ceria oxide lattice, which act as
160 oxygen storage during the CPOM reaction. On the other hand, Ni-MgO catalyst suffered from
161 the fast deactivation due to the formation of NiO/MgO solid solution, which is hardly reduced
162 under the CPOM reaction conditions [33]. Thus, acidic supports are better than basic supports in
163 CPOM reaction and in general, zeolite support performs better than alumina due to their higher

164 acidity, along with surface area. Osman et al. [13] prepared Ni on η-Al_2O_3 and ZSM-5(80) on
165 the addition of CeO_2-ZrO_2 as oxygen storage, where Ni/ CeO_2-ZrO_2/ZSM-5(80) showed higher
166 methane conversion than that of Ni/ CeO_2-ZrO_2/ η-Al_2O_3 catalyst with $T_{50\%}$ of 392 and 415 °C,
167 respectively. This was explained due to three reasons; the larger surface area, surface acidity and
168 increased interaction and interfacial area between the Ni and ZSM-5(80) compared to the η-
169 Al_2O_3 catalyst. Firstly, the larger S_{BET} and pore structure of the ZSM-5 (80) resulted in higher
170 dispersion in the catalyst pores (Ni/ CeO_2-ZrO_2/ZSM-5(80)) and a correspondingly larger
171 number of smaller Ni nanoparticles within the catalyst. Secondly, it is well known that zeolite
172 type catalysts offer strong Bronsted acidic sites, compared to the weak and medium Lewis acidic
173 sites in alumina type catalysts. Thus, ZSM-5(80) increased the electrophilicity of the Ni metal
174 and consequently enhanced the re-oxidation step in the catalytic cycle during the CPOM reaction,
175 accordingly, increasing the rate of the reaction. Thirdly, the increased acidity led to strong
176 interaction and increased the interfacial area between the Ni and the ZSM-5(80) support which
177 boosted the oxygen transfer from the oxygen storage (CeO_2-ZrO_2) and ZSM-5(80) support onto
178 the Ni metal for its re-oxidation and also the oxidation of any carbon atom deposited on the
179 surface of the catalyst into CO or CO_2, thus removal of the coke [13]. 5%Ni/$Ce_{0.25}$-$Zr_{0.75}O_2$
180 catalyst was used in CPOM reaction with a $T_{50\%}$ of 550 °C and CO selectivity of 90% at 750 °C
181 (GHSV of 106,000 $ml.g^{-1}.h^{-1}$) [37]. However, most oxygen storage materials such as CeO_2, ZrO_2
182 or a mixture of both intrinsically offer low surface area along with a high associated cost.
183 Therefore, they are not preferred to be used as a single support. Consequently, to overcome this,
184 many studies added alumina as dual support along with the oxygen storage due to their high
185 surface area and their low cost [20, 38]. For instance, a substantial increase in the catalytic
186 activity was found for the Ni/CeO_2-ZrO_2-Al_2O_3 catalyst with S_{BET} of 165.3 $m^2.g^{-1}$, compared to
187 that without Al_2O_3 which had S_{BET} of 25.8 $m^2.g^{-1}$ with $T_{90\%}$ at a temperature of 720 °C and
188 >800 °C, respectively (GHSV of 200,000 $mL.g^{-1}.h^{-1}$) [20]. The CO selectivity was also slightly

189 increased from 93% to 95% at reaction temperature 700 °C for Ni/CeO_2-ZrO_2 and Ni/CeO_2-
190 ZrO_2-Al_2O_3, respectively. Xiulan Cai et al.[38] examined Ni loaded on Al_2O_3, ZrO_2-Al_2O_3,
191 CeO_2-Al_2O_3 and CeO_2-ZrO_2-Al_2O_3 for methane auto-thermal reforming. The catalyst supports
192 were prepared using coprecipitation method while the 10 wt.% Ni was loaded using wetness
193 impregnation method. The results showed that the catalytic performance and stability of
194 Ni/CeO_2-ZrO_2-Al_2O_3 was the best in this particular work. The 10 wt.% Ni/Al_2O_3 catalyst showed
195 methane conversion of 73%, while Ni/CeO_2-ZrO_2-Al_2O_3 catalyst showed 93%.

196 **5. Effect of preparation methods:**
197

198 The close interaction and interfacial area between the metal, reducible oxide and acidic support
199 are crucial during the CPOM reaction, which leads to improving the catalytic performance along
200 with the catalyst stability. The close interaction is required to allow better interaction between
201 the metal and the oxygen vacancies on the support, which not only improves the redox behaviour
202 of the metal during the COPM reaction cycle, but also supplies oxygen to facilitate the oxidation
203 and removal of any coke deposited. This can be achieved by preparing catalysts with very small
204 particle sizes or by using a co-precipitation method to prepare the CPOM catalysts. For example,
205 10% Ni/CeO_2 catalyst was prepared using co-precipitation method which significantly improved
206 the interaction between the CPOM catalyst components and hence, enhanced the catalytic
207 performance with a $T_{50\%}$ at 525 °C, compared with 630 °C for the catalyst prepared by
208 impregnation (GHSV of 10,400 $mL.g^{-1}.h^{-1}$) [21]. Cai et al. [38] used the co-precipitation method
209 to prepare Ni-based catalyst on different supports (Al_2O_3, ZrO_2-Al_2O_3, CeO_2-Al_2O_3 and CeO_2-
210 ZrO_2-Al_2O_3) and used these for the methane auto-thermal reforming reaction. They found out
211 that Ni/CeO_2-ZrO_2-Al_2O_3 catalyst showed good dispersion of NiO allowing improved oxygen
212 transfer, but also decreased the formation of nickel aluminate which has no catalytic activity
213 during combustion reactions. Recently, the co-precipitation method was used to prepare higher

214 S_{BET} CPOM catalyst than the equivalent catalysts prepared with a wet-impregnation method for
215 both alumina and ZSM-5 (80) support [13]. The CO-chemisorption test also revealed that the co-
216 precipitation method offered higher Ni dispersion than that of the wet-impregnation method. The
217 catalytic activity of zeolite catalysts, 10% Ni/ CeO_2-ZrO_2/ZSM-5 (80) using co-precipitation and
218 wet-impregnation methods showed $T_{50\%}$ at 392 and 415 °C, respectively. Ozdemir et al.[39]
219 studied the effect of the calcination temperature along with the time of the calcination on
220 Ni/$MgAl_2O_4$ catalyst for CPOM reaction. They reported that the calcination temperature (500-
221 1000 °C for 3hrs) improved the metal oxide support interaction, but calcination time only caused
222 the catalyst sintering (1000 °C for 10 hrs). Moreover, the higher ratio of basicity to acidity
223 increased with increasing the calcination temperature and inhibited the amount of coke
224 deposition on the catalyst due to the enhanced CO_2 chemisorption. They also found that coke
225 deposition increased with increasing the Ni particle size [39].

226 **6. Reaction mechanism**
227

228 There are mainly two mechanisms for CPOM reaction where there are several factors affecting
229 the reaction mechanisms such as the catalyst components, reaction conditions and the interaction
230 between the metals and support within the catalyst [26, 30, 40-45]. The first mechanism is the
231 direct partial oxidation (DPO) which involves the dissociation of CH_4 followed by oxidation of
232 surface carbon to CO and subsequent desorption of CO and H_2 gases as shown in Figure 1 (a).
233 The combustion and reforming reaction (CRR) mechanism involves the complete combustion of
234 CH_4 into combustion products (CO_2 and H_2O), which are then converted through dry or steam
235 reforming to CO and H_2 as shown in Figure 1 (b).

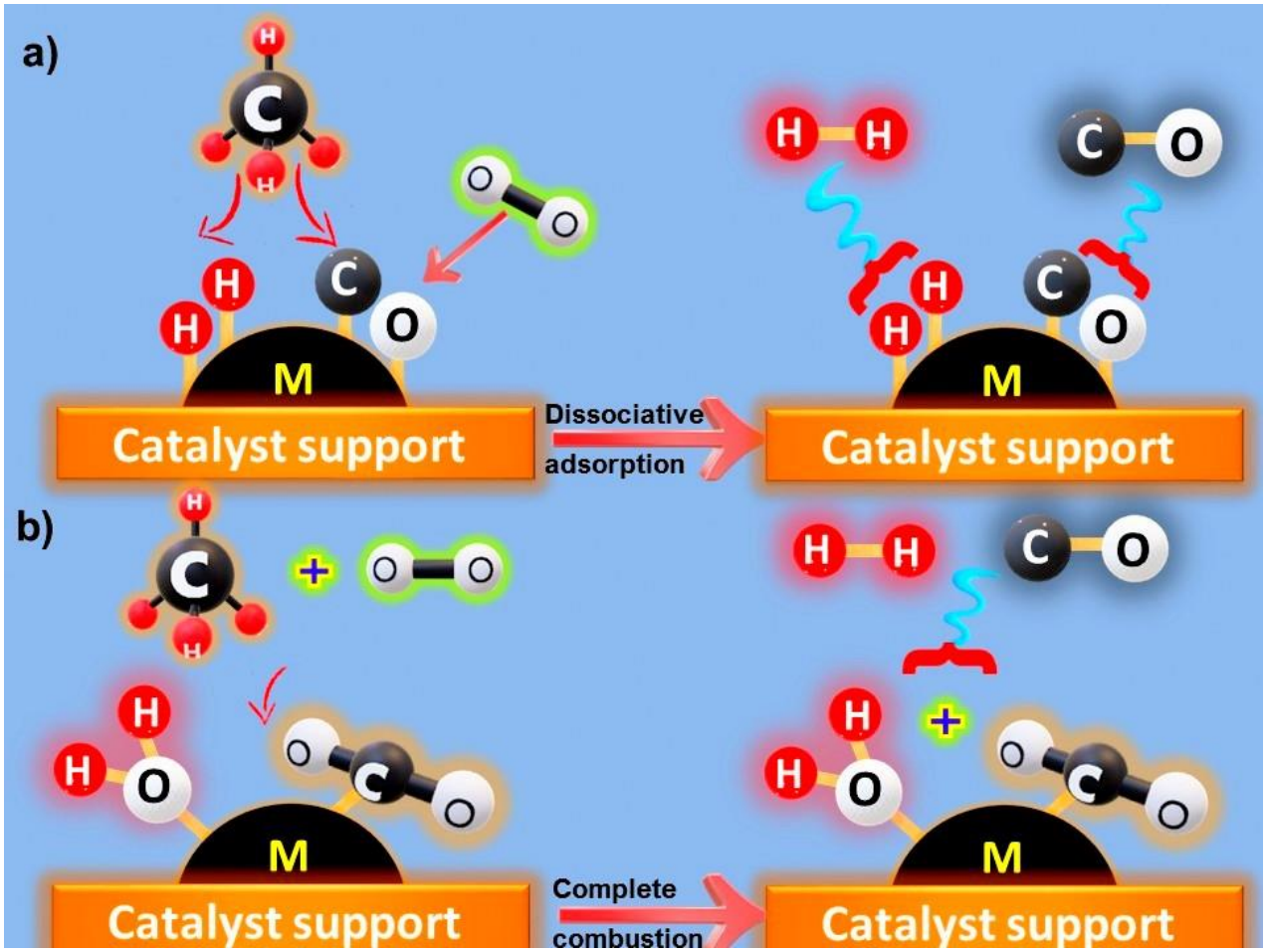

Figure 1: shows the two reaction mechanisms involved in the catalytic partial oxidation of methane (a, b).

In TMO reaction mechanism, CH_4 is dissociatively adsorbed on the metal and the methyl species are then fully oxidised by PdO present on the surface. The resulting reduced metal species is then oxidised by the lattice oxygen from the oxygen storage such as (TiO_2 and CeO_2-ZrO_2) or from the gas phase oxygen in the reaction stream [46]. Thus, the total methane oxidation mechanism is similar to the DPO mechanism. Lanza et al. [30] studied the CPOM reaction mechanism over Pt-Ru catalyst using alumina, ceria and zirconia as catalyst supports in the temperature range of 300-800 °C and GHSV of 25000-100000 h^{-1}. They reported that Pt-Ru catalysts support the indirect route which is the CRR mechanism where combustion occurred followed by reforming reactions. However, by increasing the O_2 in the reaction feed over the stoichiometric ratio of

CPOM reaction, the combustion products were increased at low reaction temperature, thus increased the CO_2 selectivity over the CO selectivity [30]. Tavazzi et al. also proposed the CRR mechanism on Rh/α-Al_2O_3 catalyst [47]. On the other hand, recently, Osman et al. [13] reported a DPO mechanism on Ni-based catalyst for CPOM reaction.

7. Kinetic studies

The theoretical thermodynamic equilibrium calculations of different % CH_4 in the reaction are shown in Figure 2, where the low CH_4 concentration was composed of 10% CH_4, 5% O_2, 5% Ne and 80% Ar (feed A). While the high CH_4 concentration was 20% CH_4, 10% O_2, 5% Ne and 65% Ar (feed B). By taking in consideration of the formation of coke during the reaction, the selectivity of the coke decreased with increasing the reaction temperature as shown in Figure 2 (a, d) and Table 1, regardless of the methane concentration in the reaction feed. The coke selectivities in feed A, at reaction temperatures of 250, 515, 705 and 800 °C were 77, 57, 10.5 and 2%, respectively, as shown in Table 1. In general, the coke formation slightly increased by increasing the methane concentration from 10 CH_4% (feed A) into 20 CH_4% (feed B) with a dramatic increase at high reaction temperatures. For instance, the coke selectivity in feed B, at reaction temperatures of 250, 515, 705 and 800 °C were 77, 62, 21 and 8%, respectively, as shown in Table 1. The CO_2 selectivity for both feeds (A and B) showed a slight increase in the reaction temperature range of 250-500 °C, followed by a dramatic decrease in the temperature range of 550-800 °C where feed B had higher CO_2 selectivity in general as shown in Figure 2 (a, d) and Table 1. The CO_2 selectivities in feed A, at reaction temperatures of 250, 515, 705 and 800 °C were 22.9, 27.2, 5.7 and 1.2%, respectively. While at same reaction temperatures for feed B were 22.9, 27.5, 9.1 and 2.4%, respectively. On the other hand, the CO selectivity decreased with increasing the reaction temperature, with a rapid decrease in the temperature range of 477-800 °C, regardless of the methane concentration in the reaction feed where feed A had higher

selectivity in general as shown in Figure 2 (a, d). The CO selectivities in feed A, at reaction temperatures of 250, 515, 705 and 800 °C were 0.02, 15.7, 83.7 and 96.6%, respectively. While at same reaction temperatures for feed B were 0.02, 10.5, 70.3 and 89.7%, respectively, as shown in Table 1. The molar fraction of the reaction products are shown in Figure 2 (b, e) and Table 1. Firstly, Ne inert gas was used as an internal standard, thus its concentration remains constant, while the oxygen concentration in partial oxidation reaction is totally used in the reaction, thus its molar fraction in the products is zero. The molar fractions of CO and H_2 increased with increasing the reaction temperature while the opposite is occurring for H_2O and CH_4, as shown in Figure 2 (b, e) and Table 1. Figure 2 (c, f) shows the methane and oxygen conversions for feed A and B. It is not surprising that the O_2 conversion is always 100% in the reaction temperature range of 250-800 °C. Furthermore, by increasing the methane concentration in the reaction feed from 10 CH_4% (feed A) into 20 CH_4% (feed B), the CH_4 conversion decreased. The CH_4 conversion in feed A, at reaction temperatures of 250, 515, 705 and 800 °C were 43.6, 79.8, 96.5 and 98.6%, respectively, while at the same reaction temperatures for feed B were 42.0, 73.1, 94.3 and 97.6 %, respectively as shown in Figure 2 (c, f).

298

299 **Table 1:** The theoretical thermodynamic equilibrium selectivity and product mole fraction of

300 different methane concentrations in the reaction feed.

Reaction Temp.	*%CH_4 in feed*	*% selectivity*			*Products mole fraction*					
		CO	CO_2	Coke	CO	H_2	CO_2	H_2O	CH_4	Ar
250 °C	10% CH_4*	0.02	22.93	77.05	0.0	0.01	0.01	0.08	0.06	0.81
	20% CH_4**	0.02	22.94	77.04	0.00	0.01	0.02	0.17	0.11	0.66
515 °C	10% CH_4*	15.7	27.2	57.1	0.01	0.11	0.02	0.04	0.02	0.76
	20% CH_4**	10.52	27.5	61.96	0.02	0.17	0.04	0.09	0.05	0.60
705 °C	10% CH_4*	83.75	5.76	10.49	0.07	0.16	0.00	0.01	0.00	0.71
	20% CH_4**	70.31	9.07	20.62	0.11	0.28	0.01	0.02	0.01	0.53
800 °C	10% CH_4*	96.58	1.25	2.17	0.08	0.17	0.00	0.00	0.00	0.71
	20% CH_4**	89.71	2.39	7.90	0.14	0.30	0.00	0.01	0.00	0.51

301
302 *Feed A is the reaction feed composition of (10% CH_4 + 5% O_2 + 5% Ne + 80% Ar)
303 ** Feed B is the reaction feed composition of (20% CH_4 + 10% O_2 + 5% Ne + 65% Ar)

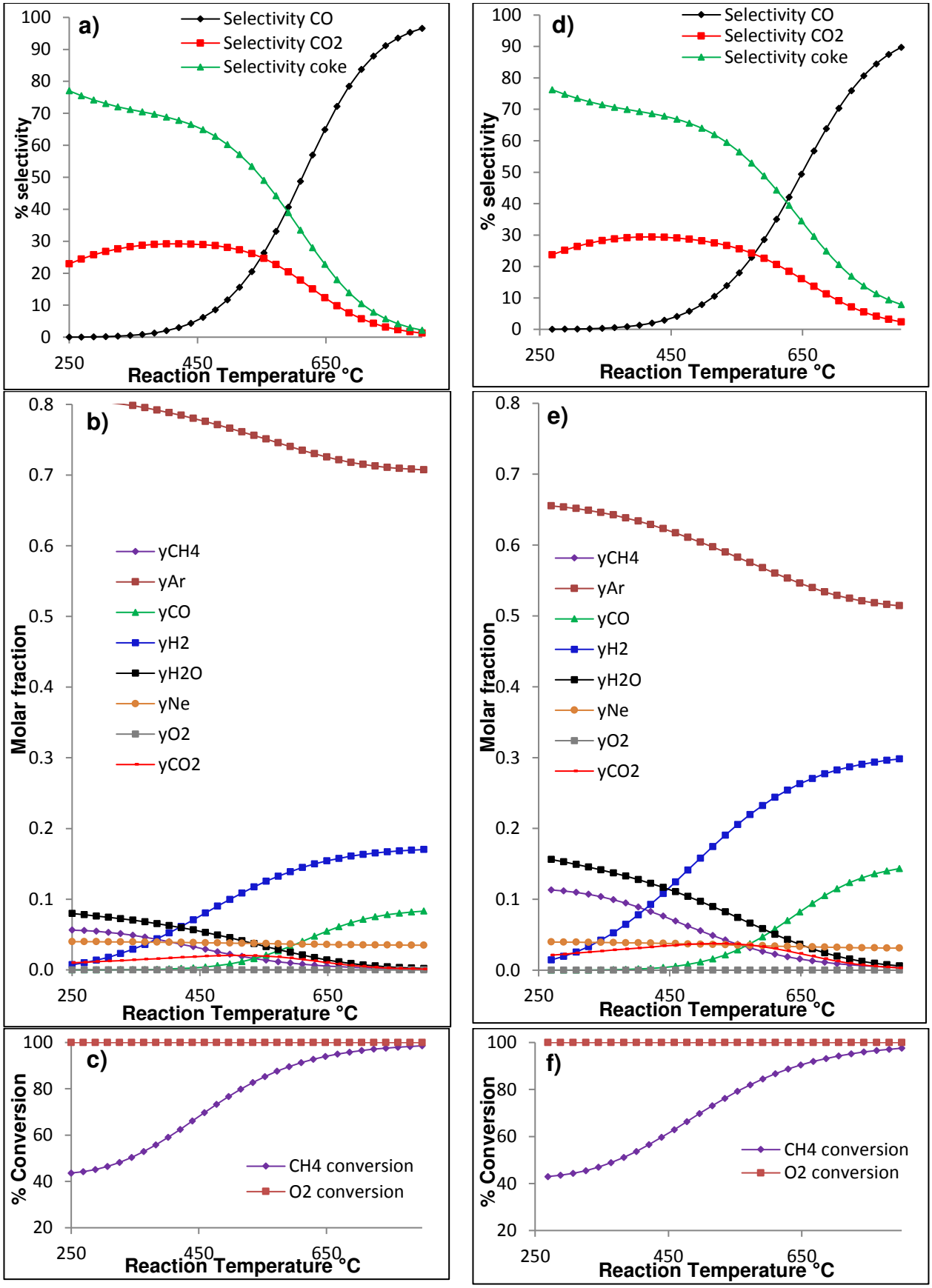

304 **Figure 2:** Theoretical thermodynamic equilibrium calculations of different % CH_4 in the feed
305 10% CH_4 (left) and 20% CH_4 (right): selectivity (a, d), fraction yield (b, e) and conversion (c, f).

8. Deactivation of CPOM catalysts

As shown in Figure 2 that the coke selectivity is higher at lower reaction temperatures which is one of the main reason for catalyst deactivation in CPOM reaction. It is well known that the produced CO adsorbs strongly over the surface of the catalyst at the lower reaction temperature, leading to reversibility deactivate the catalyst. In previous work, CO was added to the reaction stream as shown in Figure 3, where the extent of CO poisoning increased with decreasing the reaction temperature. For instance, at a reaction temperature of 600 °C, the % methane conversion decreased from 83 to 79%. While at a reaction temperature of 400 °C, there was a significant decrease of 10% in the methane conversion from approximately 52 to 42% as shown in Figure 3. Thus having oxygen storage such as reducible oxide support helps to re-oxidise and clean the surface of the catalyst. On the other hand, molybdenum phosphide is being used in methane dry and oxy-reforming (partial oxidation) where MoP is the dominant active site and it deactivates due to the bulk oxidation [48]. The MoP catalyst deactivates gradually when it converted into the less active phase molybdenum carbide (Mo_2C) then a rapid deactivation due to the bulk oxidation into the non-active phase of MoO_2. Cui et al. also reported that due to the higher H_2 yield in CPOM reaction compared to dry reforming which maintains the redox cycle of the MoP catalyst, thus showed higher catalytic stability [48]. Recently, Karaismailoglu et al.[49] studied the effect of doping yttria oxide (Y_2O_3) doped nickel-based catalyst on methane decomposition. They found out the pure Ni-based catalyst suffers from rapid deactivation due to coke formation while loading yttria oxide helps to improve the catalytic activity and reduce the carbon deposition. One of the main factors of deactivating nickel-based catalyst is the formation of nickel aluminate.

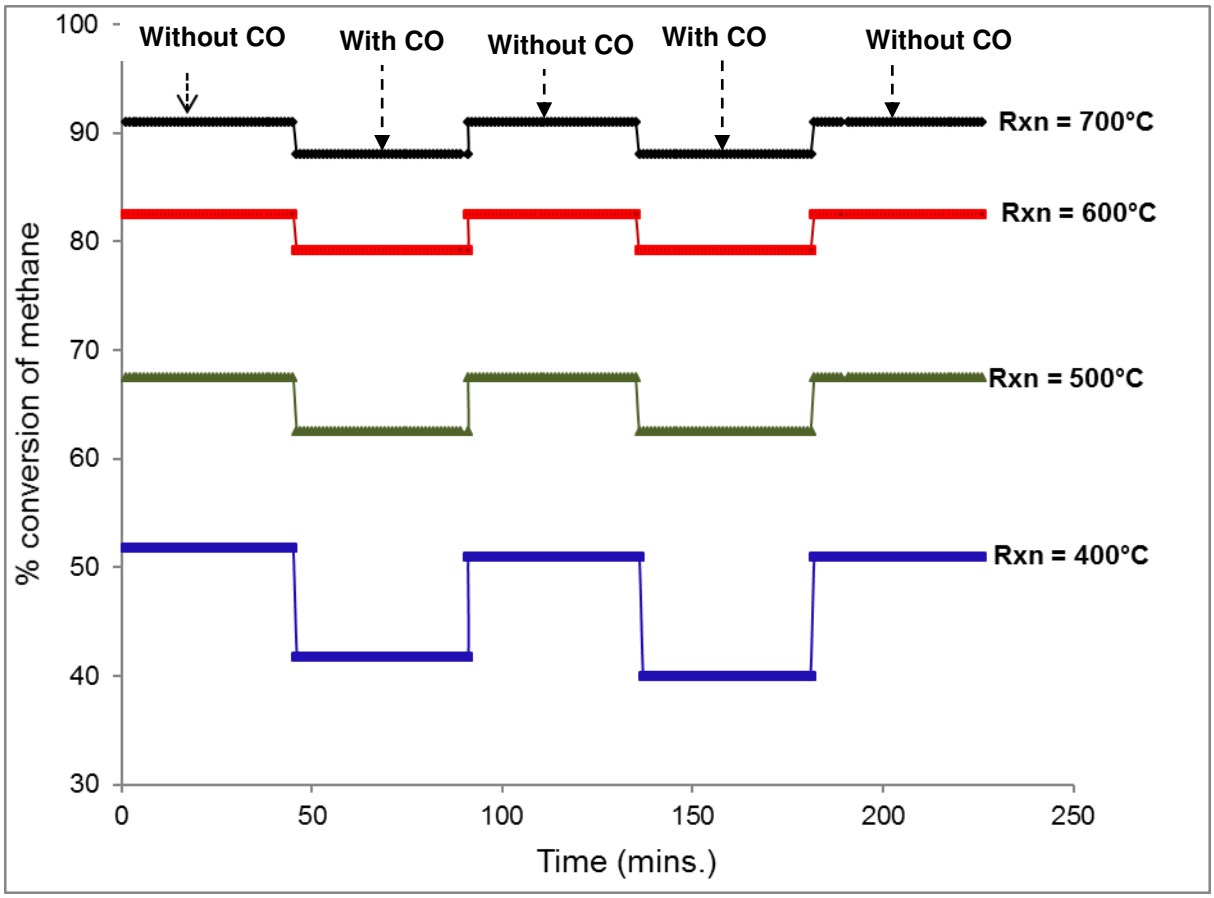

Figure 3: The inhibition effect of CO added to the CPOM reaction feed. Reaction conditions: temperature, 400-700 °C with WHSV, 63000 mL.g^{-1} h^{-1} [13].

9. Conclusion

Nickel is recognised as one of the cheapest and most active transition metal catalysts and rhodium as a noble metal. However, Ni is more prone to carbon deposition which poisons and consequently deactivates the catalyst. However, recent studies showed that nickel loaded on dual supports including a reducible metal oxide such as TiO_2 or CeO_2-ZrO_2, which act as oxygen storage and re-oxidise any coke deposition, thus clean-up the catalyst and enhance its stability. The acidity in zeolite or alumina supports enhances the reoxidation of the metal catalyst, thus enhancing the redox cycle during the CPOM reaction. Therefore, the three main components; the metal, reducible mixed oxide and acidic catalyst support are crucial in CPOM reaction along with the close interaction and interfacial area between the catalyst components for the catalyst activity and stability. However, this is not the case for molybdenum phosphide catalysts in the reforming reactions, where MoP is the dominant active site and it deactivates due to the bulk oxidation. Given the fact of the close interaction, the co-precipitation offered better and close interaction between the active components than the wet-impregnation method. The extent of the reversible CO poisoning increased with decreasing the reaction temperature during the CPOM reaction. Bimetallic catalysts showed better stability than a single metal catalyst such as Pt stabilises the Pd metal in total methane oxidation or Y_2O_3 stabilises Ni-based catalysts in CPOM reaction.

Acknowledgement: The author would like to acknowledge the support given by the EPSRC project "Advancing Creative Circular Economies for Plastics via Technological-Social Transitions" (ACCEPT Transitions, EP/S025545/1). AO wish to acknowledge the support of Professor David Rooney, the director of the Sustainable Energy Research Centre, at Queen's University Belfast. The author also wish to acknowledge the support of The Bryden Centre project (Project ID VA5048) which was awarded by The European Union's INTERREG VA Programme, managed by the Special EU Programmes Body (SEUPB), with match funding provided by the Department for the Economy in Northern Ireland and the Department of Business, Enterprise and Innovation in the Republic of Ireland. The authors would like to thank Charlie Farrell and Patrick McNicholl who assisted in the proof-reading of the manuscript.

Competing financial interests: The author declares no competing financial interests.

Symbols and abbreviations

Abbreviation and nomenclature			
Catalytic partial oxidation of methane	*CPOM*	**Methane total oxidation**	*MTO*
Combustion and reforming reaction	*CRR*	**Molybdenum carbide**	Mo_2C
Dimethyl ether	*DME*	**Nitrogen oxide**	NO_x
Direct partial oxidation	*DPO*	**Sulfur oxide**	SO_x
Gas hourly space velocity	*GHSV*	**Water gas shift reaction**	*WGSR*
Greenhouse gas	*GHG*	**Yttria oxide**	Y_2O_3

References

[1] R. Horn, R. Schlogl, *Catalysis Letters*, **2015**, *145 (1),* 23-39. DOI: 10.1007/s10562-014-1417-z

[2] P. Weiland, *Applied Microbiology and Biotechnology*, journal article, **2010**, *85 (4),* 849-860. DOI: 10.1007/s00253-009-2246-7

[3] Center for Climate and Energy Solutions, Leveraging Natural Gas to Reduce Greenhouse Gas Emissions, URL: http://www.c2es.org/publications/leveraging-natural-gas-reduce-greenhouse-gas-emissions **2013,** accessed 3-12-2019.

[4] B. Christian Enger, R. Lodeng, A. Holmen, *Applied Catalysis A: General*, **2008**, *346 (1-2),* 1-27. DOI: http://dx.doi.org/10.1016/j.apcata.2008.05.018

[5] G. Pantaleo, V. La Parola, F. Deganello, P. Calatozzo, R. Bal, A. M. Venezia, *Applied Catalysis B: Environmental*, **2015**, *164,* 135-143. DOI: http://dx.doi.org/10.1016/j.apcatb.2014.09.011

[6] J. A. Velasco, C. Fernandez, L. Lopez, S. Cabrera, M. Boutonnet, S. Jaras, *Fuel*, **2015**, *153,* 192-201. DOI: http://dx.doi.org/10.1016/j.fuel.2015.03.009

[7] J. Kagawa, *Toxicology*, **2002**, *181–182,* 349-353. DOI: http://dx.doi.org/10.1016/S0300-483X(02)00461-4

[8] V. N. Nguyen, L. Blum, *Chemie Ingenieur Technik*, **2015**, *87 (4),* 354-375. DOI: 10.1002/cite.201400090

[9] S. Adamu, Q. Xiong, I. A. Bakare, M. M. Hossain, *International Journal of Hydrogen Energy*, Article, **2019**, *44 (30),* 15811-15822. DOI: 10.1016/j.ijhydene.2018.12.136

[10] A. I. Osman, J. K. Abu-Dahrieh, D. W. Rooney, S. A. Halawy, M. A. Mohamed, A. Abdelkader, *Applied Catalysis B: Environmental*, **2012**, *127,* 307-315. DOI: http://dx.doi.org/10.1016/j.apcatb.2012.08.033

[11] A. I. Osman, J. K. Abu-Dahrieh, N. Cherkasov, J. Fernandez-Garcia, D. Walker, R. I. Walton, D. W. Rooney, E. Rebrov, *Molecular Catalysis*, **2018**, *455,* 38-47. DOI: https://doi.org/10.1016/j.mcat.2018.05.025

[12] J. R. Rostrup-Nielsen, *Catalysis Today*, **2002**, *71 (3–4),* 243-247. DOI: http://dx.doi.org/10.1016/S0920-5861(01)00454-0

[13] A. I. Osman, J. Meudal, F. Laffir, J. Thompson, D. Rooney, *Applied Catalysis B: Environmental*, **2017**, *212,* 68-79. DOI: https://doi.org/10.1016/j.apcatb.2016.12.058

[14] A. C. W. Koh, L. Chen, W. Kee Leong, B. F. G. Johnson, T. Khimyak, J. Lin, *International Journal of Hydrogen Energy*, **2007**, *32 (6),* 725-730. DOI: http://dx.doi.org/10.1016/j.ijhydene.2006.08.002

[15] E. C. Faria, R. C. R. Neto, R. C. Colman, F. B. Noronha, *Catalysis Today*, **2014**, *228,* 138-144. DOI: http://dx.doi.org/10.1016/j.cattod.2013.10.058

[16] W.-S. Dong, H.-S. Roh, K.-W. Jun, S.-E. Park, Y.-S. Oh, *Applied Catalysis A: General*, **2002**, *226 (1-2),* 63-72. DOI: http://dx.doi.org/10.1016/S0926-860X(01)00883-3

[17] A. Scarabello, D. Dalle Nogare, P. Canu, R. Lanza, *Applied Catalysis B: Environmental*, **2015**, *174-175,* 308-322. DOI: http://dx.doi.org/10.1016/j.apcatb.2015.03.012

[18] A. J. de Abreu, A. F. Lucredio, E. M. Assaf, *Fuel Processing Technology*, **2012**, *102,* 140-145. DOI: http://dx.doi.org/10.1016/j.fuproc.2012.04.030

[19] T. Mondal, K. K. Pant, A. K. Dalai, *International Journal of Hydrogen Energy*, **2015**, *40 (6),* 2529-2544. DOI: http://dx.doi.org/10.1016/j.ijhydene.2014.12.070

[20] M. Dajiang, C. Yaoqiang, Z. Junbo, W. Zhenling, M. Di, G. Maochu, *Journal of Rare Earths*, **2007**, *25 (3),* 311-315. DOI: http://dx.doi.org/10.1016/S1002-0721(07)60428-1

[21] S. Xu, X. Wang, *Fuel*, **2005**, *84 (5),* 563-567. DOI: http://dx.doi.org/10.1016/j.fuel.2004.10.008

[22] Y. Wang, J. Peng, C. Zhou, Z.-Y. Lim, C. Wu, S. Ye, W. G. Wang, *International Journal of Hydrogen Energy*, **2014**, *39 (2),* 778-787. DOI: http://dx.doi.org/10.1016/j.ijhydene.2013.10.071
[23] S. Rabe, T.-B. Truong, F. Vogel, *Applied Catalysis A: General*, **2005**, *292,* 177-188. DOI: http://dx.doi.org/10.1016/j.apcata.2005.06.001
[24] S. R. Deshmukh, D. G. Vlachos, *Combustion and Flame*, **2007**, *149 (4),* 366-383. DOI: http://dx.doi.org/10.1016/j.combustflame.2007.02.006
[25] S. A. Al-Sayari, *The Open Catalysis Journal* **2013**, *6,* 17-28. DOI: 10.2174/1876214X20130729001
[26] R. Horn, K. A. Williams, N. J. Degenstein, A. Bitsch-Larsen, D. Dalle Nogare, S. A. Tupy, L. D. Schmidt, *Journal of Catalysis*, **2007**, *249 (2),* 380-393. DOI: http://dx.doi.org/10.1016/j.jcat.2007.05.011
[27] S. Ren, Y. Zhang, Y. Liu, T. Sakao, D. Huisingh, C. M. V. B. Almeida, *Journal of Cleaner Production*, **2019**, *210,* 1343-1365. DOI: https://doi.org/10.1016/j.jclepro.2018.11.025
[28] A. I. Osman, J. K. Abu-Dahrieh, F. Laffir, T. Curtin, J. M. Thompson, D. W. Rooney, *Applied Catalysis B: Environmental*, **2016**. DOI: http://dx.doi.org/10.1016/j.apcatb.2016.01.017
[29] T. H. Nguyen, A. Łamacz, A. Krztoń, A. Ura, K. Chałupka, M. Nowosielska, J. Rynkowski, G. Djéga-Mariadassou, *Applied Catalysis B: Environmental*, **2015**, *165,* 389-398. DOI: http://dx.doi.org/10.1016/j.apcatb.2014.10.019
[30] R. Lanza, P. Canu, S. G. Järås, *Applied Catalysis A: General*, **2010**, *375 (1),* 92-100. DOI: https://doi.org/10.1016/j.apcata.2009.12.021
[31] A. I. Osman, J. K. Abu-Dahrieh, M. McLaren, F. Laffir, D. W. Rooney, *ChemistrySelect*, **2018**, *3 (5),* 1545-1550. DOI: 10.1002/slct.201702660
[32] V. N. Rogozhnikov, P. V. Snytnikov, A. N. Salanov, A. V. Kulikov, N. V. Ruban, D. I. Potemkin, V. A. Sobyanin, V. V. Kharton, *Materials Letters*, **2019**, *236,* 316-319. DOI: https://doi.org/10.1016/j.matlet.2018.10.133
[33] C. Alvarez-Galvan, M. Melian, L. Ruiz-Matas, J. L. Eslava, R. M. Navarro, M. Ahmadi, B. Roldan Cuenya, J. L. G. Fierro, *Frontiers in Chemistry*, Original Research, **2019**, *7 (104)*. DOI: 10.3389/fchem.2019.00104
[34] Z. Boukha, M. Gil-Calvo, B. de Rivas, J. R. González-Velasco, J. I. Gutiérrez-Ortiz, R. López-Fonseca, *Applied Catalysis A: General*, **2018**, *556,* 191-203. DOI: https://doi.org/10.1016/j.apcata.2018.03.002
[35] H. E. Figen, S. Z. Baykara, *International Journal of Hydrogen Energy*, **2015**, *40 (24),* 7439-7451. DOI: http://dx.doi.org/10.1016/j.ijhydene.2015.02.109
[36] C. Cheephat, P. Daorattanachai, S. Devahastin, N. Laosiripojana, *Applied Catalysis A: General*, **2018**, *563,* 1-8. DOI: https://doi.org/10.1016/j.apcata.2018.06.032
[37] A. S. Larimi, S. M. Alavi, *Fuel*, **2012**, *102,* 366-371. DOI: http://dx.doi.org/10.1016/j.fuel.2012.06.050
[38] X. Cai, Y. Cai, W. Lin, *Journal of Natural Gas Chemistry*, **2008**, *17 (2),* 201-207. DOI: http://dx.doi.org/10.1016/S1003-9953(08)60052-3
[39] H. Ozdemir, M. A. F. Oksüzömer, M. A. Gurkaynak, *Fuel*, **2014**, *116,* 63-70. DOI: http://dx.doi.org/10.1016/j.fuel.2013.07.095
[40] R. Jin, Y. Chen, W. Li, W. Cui, Y. Ji, C. Yu, Y. Jiang, *Applied Catalysis A: General*, **2000**, *201 (1),* 71-80. DOI: http://dx.doi.org/10.1016/S0926-860X(00)00424-5
[41] A. G. Steghuis, J. G. van Ommen, J. A. Lercher, *Catalysis Today*, **1998**, *46 (2–3),* 91-97. DOI: http://dx.doi.org/10.1016/S0920-5861(98)00330-7
[42] C. Ding, J. Wang, Y. Jia, G. Ai, S. Liu, P. Liu, K. Zhang, Y. Han, X. Ma, *International Journal of Hydrogen Energy*, **2016**, *41 (25),* 10707-10718. DOI: http://dx.doi.org/10.1016/j.ijhydene.2016.04.110

[43] D. A. Hickman, L. D. Schmidt, *Journal of Catalysis*, **1992**, *138 (1),* 267-282. DOI: http://dx.doi.org/10.1016/0021-9517(92)90022-A
[44] R. Horn, K. A. Williams, N. J. Degenstein, L. D. Schmidt, *Journal of Catalysis*, **2006**, *242 (1),* 92-102. DOI: http://dx.doi.org/10.1016/j.jcat.2006.05.008
[45] W. Z. Weng, M. S. Chen, Q. G. Yan, T. H. Wu, Z. S. Chao, Y. Y. Liao, H. L. Wan, *Catalysis Today*, **2000**, *63 (2–4),* 317-326. DOI: http://dx.doi.org/10.1016/S0920-5861(00)00475-2
[46] J. N. Carstens, S. C. Su, A. T. Bell, *Journal of Catalysis*, **1998**, *176 (1),* 136-142. DOI: http://dx.doi.org/10.1006/jcat.1998.2029
[47] I. Tavazzi, A. Beretta, G. Groppi, P. Forzatti, *Journal of Catalysis*, **2006**, *241 (1),* 1-13. DOI: https://doi.org/10.1016/j.jcat.2006.03.018
[48] Y. Cui, Q. Liu, Z. Yao, B. Dou, Y. Shi, Y. Sun, *International Journal of Hydrogen Energy*, **2019**, *44 (23),* 11441-11447. DOI: https://doi.org/10.1016/j.ijhydene.2019.03.170
[49] M. Karaismailoglu, H. E. Figen, S. Z. Baykara, *International Journal of Hydrogen Energy*, **2019**, *44 (20),* 9922-9929. DOI: https://doi.org/10.1016/j.ijhydene.2018.12.214

Figure and Table legends:

Figure 1: shows the two reaction mechanisms involved in the catalytic partial oxidation of methane (a, b).

Figure 2: Theoretical thermodynamic equilibrium calculations of different % CH_4 in the feed 10% CH_4 (left) and 20% CH_4 (right): selectivity (a, d), fraction yield (b, e) and conversion (c, f).

Figure 3: The inhibition effect of CO added to the CPOM reaction feed. Reaction conditions: temperature, 400-700 °C with WHSV, 63000 $mL.g^{-1}\,h^{-1}$ [13].

Table 1: The theoretical thermodynamic equilibrium selectivity and product mole fraction of different methane concentrations in the reaction feed.

Short text for the table of contents section

Herein, the mini-review investigates the multifunctional potential of a transition and noble metal catalyst supported on either single support or combined oxide support in the catalytic partial oxidation of methane. The factors that influence the oxidation reaction along with the mechanism and the kinetic studies were also reported. The main reasons for catalyst deactivation were also explored.

515 **Table of Contents (TOC)**

516

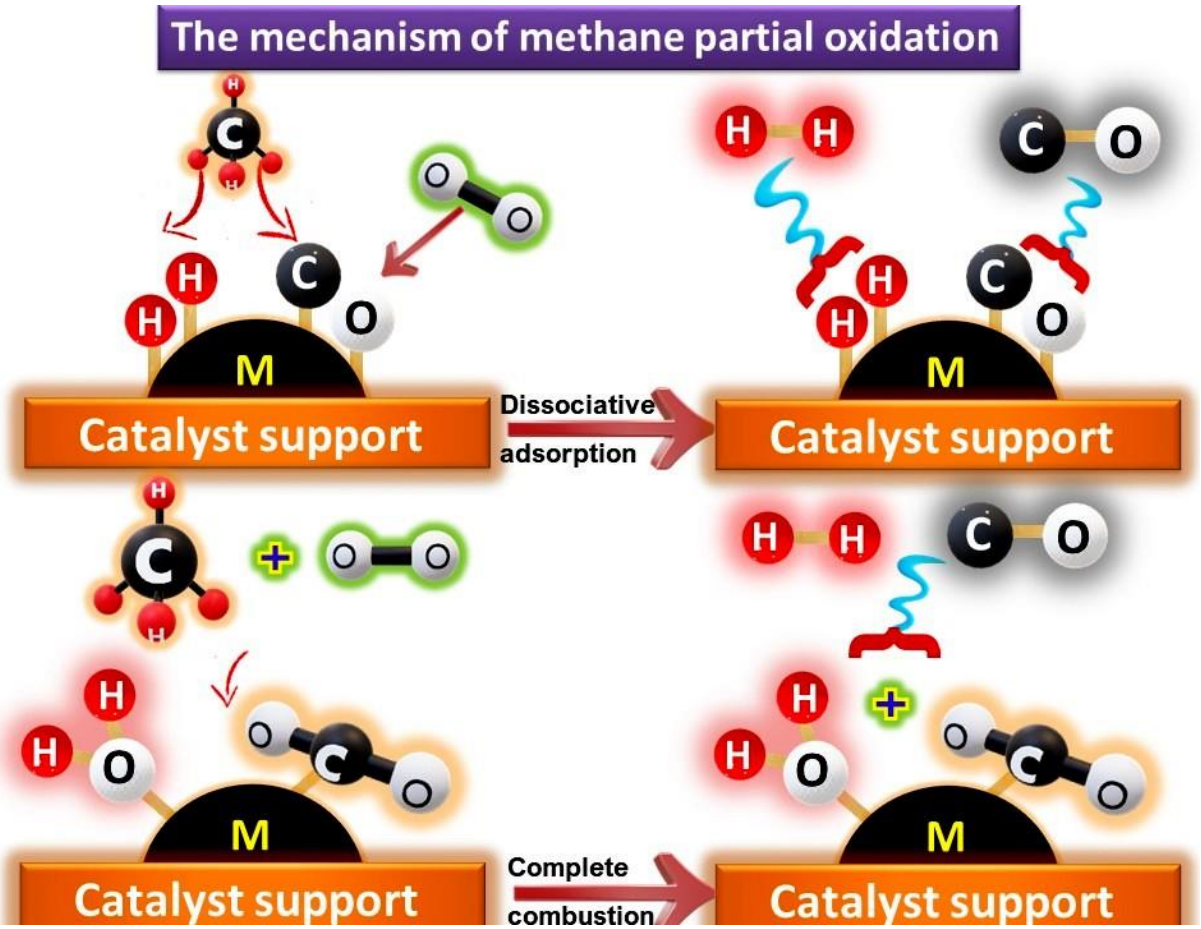

517

518

519

520

521

522